


RESEARCH ARTICLE

An injectable gelatin/sericin hydrogel loaded with human umbilical cord mesenchymal stem cells for the treatment of uterine injury

Lixuan Chen^{1,2} | Ling Li³ | Qinglin Mo⁴ | Xiaomin Zhang^{1,2} | Chaolin Chen⁴ |
Yingnan Wu⁴ | Xiaoli Zeng⁵ | Kaixian Deng⁶ | Nanbo Liu⁷ | Ping Zhu⁷ |
Mingxing Liu⁸ | Yang Xiao^{1,9} 

¹Guangzhou University of Chinese Medicine, Guangzhou, Guangdong, China

²Jinshazhou Hospital of Guangzhou University of Chinese Medicine, Guangzhou, Guangdong, China

³Jiangmen Maternity and Child Health Care Hospital, Jiangmen, Guangdong, China

⁴Translational Medicine Center, The Second Affiliated Hospital of Guangzhou Medical University, Guangzhou, Guangdong, China

⁵National Seed Cell Bank of South China for Tissue Engineering, Guangzhou, Guangdong, China

⁶Department of Gynecology, Shunde Hospital, Southern Medical University (The First People's Hospital of Shunde), Foshan, Guangdong, China

⁷Guangdong Cardiovascular Institute, Guangdong Provincial People's Hospital, Guangdong Academy of Medical Sciences, Guangzhou, China

⁸Department of Obstetrics and Gynecology, Key Laboratory for Major Obstetric Diseases of Guangdong Province, The Third Affiliated Hospital of Guangzhou Medical University, Guangzhou, Guangdong, China

⁹Shenzhen Qianhai Shekou Pilot Free Trade Zone Hospital, Shekou, Shenzhen, Guangdong, China

Correspondence

Ping Zhu, Guangdong Cardiovascular Institute, Guangdong Provincial People's Hospital, Guangdong Academy of Medical Sciences, Guangzhou 510100, China.
Email: tanganqier@163.com

Mingxing Liu, Department of Obstetrics and Gynecology, Guangdong Provincial Key Laboratory of Major Obstetric Diseases, The Third Affiliated Hospital of Guangzhou Medical University, Guangzhou, China.
Email: 2009683032@gzhu.edu.cn

Yang Xiao, Guangzhou University of Chinese Medicine, Guangzhou, Guangdong 510006, China; Shenzhen Qianhai Shekou Pilot Free Trade Zone Hospital, Shekou, Shenzhen, Guangdong 518101, China.
Email: jdxiao111@163.com

Funding information

Foshan Municipal Science and Technology Bureau 2020 Foshan Municipal Science and Technology Research Project, Grant/Award Number: 2020001006077; Special funding Fund for Clinical Scientific Research of Wu

Abstract

Abnormal endometrial receptivity is a major cause of the failure of embryo transplantation, which may lead to infertility, adverse pregnancy, and neonatal outcomes. While hormonal treatment has dramatically improved the fertility outcomes in women with endometriosis, a substantial unmet need persists in the treatment. In this study, methacrylate gelatin (GelMA) and methacrylate sericin (SerMA) hydrogel with human umbilical cord mesenchymal stem cells (HUMSC) encapsulation was designed for facilitating endometrial regeneration and fertility restoration through in situ injection. The presented GelMA/10%SerMA hydrogel showed appropriate swelling ratio, good mechanical properties, and degradation stability. In vitro cell experiments showed that the prepared hydrogels had excellent biocompatibility and cell encapsulation ability of HUMSC. Further in vivo experiments demonstrated that GelMA/SerMA@HUMSC hydrogel could increase the thickness of endometrium and improve the endometrial interstitial fibrosis. Moreover, regenerated endometrial tissue was more receptive to transfer embryos. Summary, we believed that GelMA/SerMA@HUMSC hydrogel will hold tremendous promise to repair or regenerate damaged endometrium.

Lixuan Chen and Ling Li contributed equally to this work.

This is an open access article under the terms of the [Creative Commons Attribution](https://creativecommons.org/licenses/by/4.0/) License, which permits use, distribution and reproduction in any medium, provided the original work is properly cited.

© 2022 The Authors. *Bioengineering & Translational Medicine* published by Wiley Periodicals LLC on behalf of The American Institute of Chemical Engineers.

Jieping Medical Foundation, Grant/Award Numbers: 320.6750.18101, 320.6750.2021-04-43; the Regional Joint Fund of basic and Applied basic Research Fund of Guangdong Province, Grant/Award Number: 2019B151520082

KEYWORDS

fertility restoration, methacrylate gelatin (GelMA), methacrylate sericin (SerMA), regeneration, stem cells, uterine injury

1 | INTRODUCTION

The uterus is one of the most important reproductive organs for women, and the endometrium (as the place for implantation, embryonic development, and pregnancy maintenance of female fertilized eggs) is the key factor for the success of pregnancy.^{1,2} However, endometrial damage was caused by physical injury (induced abortion, frequent uterine surgery) and biochemical injury (infection, endocrine disrupting chemicals), which could lead to impaired endometrial proliferation and affect embryo implantation and implantation, resulting in female infertility or repeated abortion.^{3–5} Currently, there are still big challenges for promoting the repair and regeneration of endometrium after injury. For the regeneration and repair of endometrial injury, the traditional treatment mainly includes surgical treatment, intrauterine barrier, endocrine therapy, increasing endometrial blood perfusion, and so on.^{6,7} However, the methods to promote endometrial regeneration after the moderate and severe injury are still very limited, which could not avoid endometrial regeneration disturbance and postoperative adhesion recurrence. Therefore, the key to successful treatment is the ability to prevent the reformation of uterine adhesion and promote the regeneration and repair of endometrium.

Stem cells have the pluripotency, the ability to release growth factors and regulate inflammation, which showed great potential in the treatment of a variety of injuries and diseases in regenerative medicine.^{8–10} Mesenchymal stem cells (MSCs, a kind of adult stem cells), which have the ability of stem cell proliferation and multi-directional differentiation, which could be isolated from a variety of tissues (such as umbilical cord, endometrial polyps, menstrual blood, bone marrow, adipose tissue, etc).^{11–13} Currently, a large number of animal experiments showed that MSC could improve the repair of endometrial injury and increase the pregnancy rate.^{14,15} In the mouse model of endometrial injury, intraperitoneal transplantation of endometrial mesenchymal stem cells (EnMSC) could effectively repair the damaged endometrium, increase the uterine microangiogenesis, and improve the pregnancy rate.¹⁶ Prior study proposed that intravenous injection of human umbilical cord mesenchymal stem cells (HUMSC) could increase the thickness and glands of endometrium, increase the implantation rate of embryos, reduce the excessive fibrosis, promote the vascular growth and endothelial cell proliferation, regulate the inflammatory factors, and restore the structure and function of ethanol-damaged endometrium.³ Moreover, HUMSC have the characteristics of low immunogenicity, high ability of self-replication, noninvasive collection, which could promote the regeneration and repair of injured tissue. However, there are still some shortcomings in the clinical application of MSC therapy, such as the tumorigenic potential of stem cells, thrombosis, fever, and other adverse reactions.^{17,18}

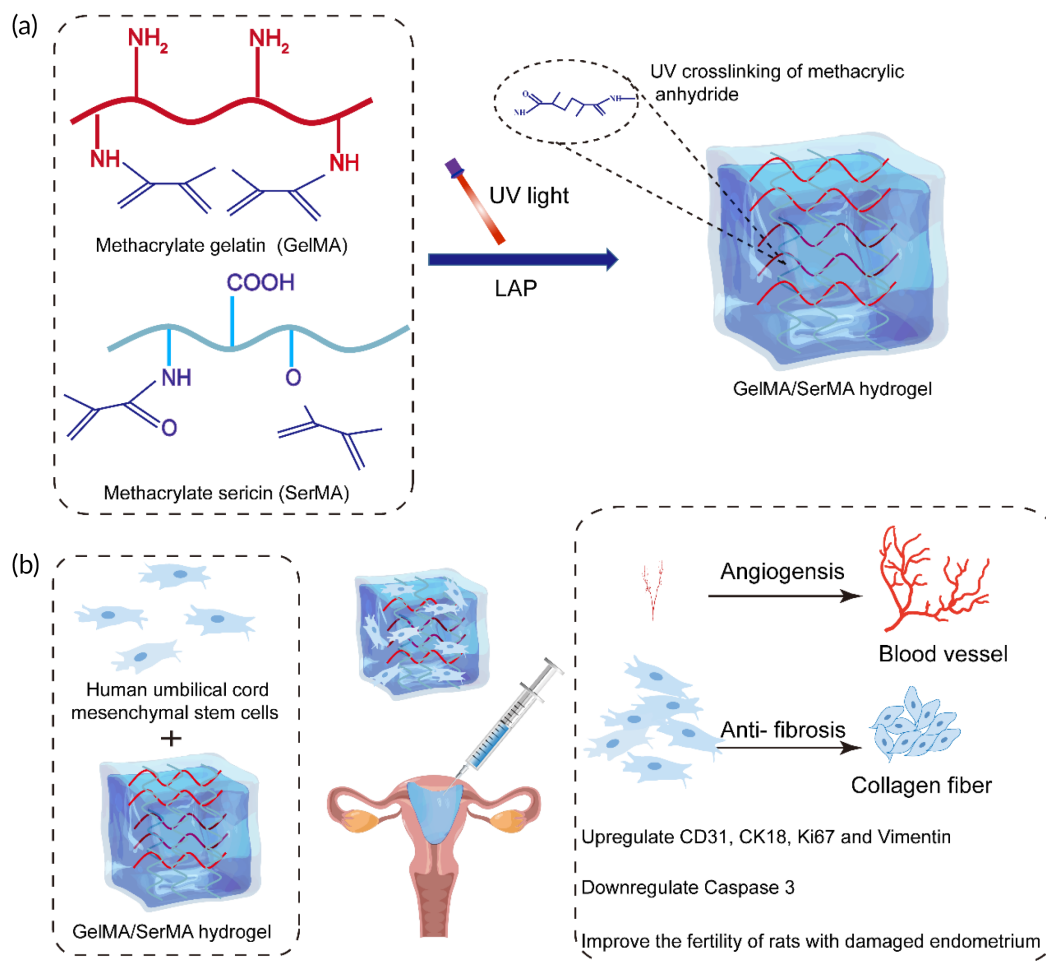
Meanwhile, the low efficiency of cell implantation caused by local injection greatly limited the clinical promotion of stem cell therapy.¹⁹

One of the main reason for the low cell retention rate is the lack of three-dimensional matrix to support the survival, migration, and development of transplanted cells.²⁰

To resolve these problems, a variety of injectable hydrogel systems have been developed, which could provide mechanical protection to prevent cell membrane from being destroyed during injection and form a stable network after injection, resulting in promoting cell adhesion and growth.^{21–25} However, many available injectable hydrogels have some problems such as poor mechanical properties, low cell survival rate, or inability to accurately control their gelation process and gel properties.^{26,27} Prior study reported that the natural extracellular matrix (ECM) environment played a key role in influencing through a series of complex physical, mechanical, and biochemical signals.^{28,29} To further understand the regulation of cell behavior by ECM, designing new materials with precise adjustable structure, mechanical properties, biodegradability, and cell interaction has been a challenging task for the research community. Therefore, our goal is to design an injectable and adjustable hydrogel crosslinked by blue or ultraviolet light to meet the different requirements of cell culture and tissue engineering applications.

Gelatin (Gel) is a derivative of collagen, which is often applied in hydrogels because of its good gelling, biocompatibility, and biodegradability.³⁰ However, one limitation of gelatin-based hydrogels is poor mechanical properties and thermal stability.³¹ These limitations can be overcome by chemical or physical cross-linking of gelatin. In addition, the addition of other ECM components can enrich gelatin hydrogels. Sericin (Ser) is a main component of natural silk and has good water solubility and excellent biocompatibility.^{32,33} Meanwhile, sericin can promote cell adhesion and proliferation, antioxidant, and inhibit tyrosinase activity.³⁴ These advantages make sericin gradually become the research focus of new natural materials in the field of tissue engineering and regenerative medicine.³⁵ In addition, the interpenetrating polymer network (IPN) hydrogel is a unique structure, which allows two independent networks to combine with each other (maintain the required properties of the original polymer) to obtain better mechanical properties.^{36,37} In this study, we hypothesized that the modified gelatin and sericin could effectively cross-link into IPN hydrogel structure, which is suitable for HUMSC cells to be incorporated into the injured tissue and play a role in tissue repair.

In this study, we aim to develop an injectable hydrogel based on methacrylate gelatin (GelMA) and methacrylate sericin (SerMA) matrix as cell delivery carriers of HUMSC to promote endometrial repair (Scheme 1). The porous structure, swelling properties, mechanical properties, and degradation properties of this hydrogel were



SCHEME 1 (a) Preparation of GelMA/SerMA hydrogel. (b) GelMA/SerMA hydrogel system encapsulating HUMSC for the treatment of uterine injury by injection into the uterine cavity

characterized. In addition, the cytocompatibility of hydrogels was studied in detail by CCK-8 and living/dead cell staining using the L929 and HUMSC cells. Meanwhile, cell encapsulation ability was characterized by three-dimensional live dead staining and cytoskeleton staining. And excellent therapeutic effect for promoting the endometrial repair and fertility restoration were shown in vivo experiments. In summary, all of these results demonstrated that the GelMA/SerMA@HUMSC hydrogel will have great potential in the repair of endometrial injury.

2 | EXPERIMENTAL SECTION

2.1 | Materials

The silkworm cocoon was obtained from the Sericultural Research Institute of Guangdong Academy of Agricultural Sciences (Guangzhou, China). Gelatin (adhesive strength ~ 500 g bloom) was purchased from the Sigma-Aldrich Chemical Company (Shanghai, China). Lithium bromide and methacrylic anhydride (MA) were obtained from Macklin Biochemical Technology Co., Ltd. (Shanghai, China). Lithium

phenyl-2,4,6-trimethylbenzoylphosphinate (LAP) was obtained from Suzhou Intelligent Manufacturing Research Institute (Suzhou, China). Human umbilical cord mesenchymal stem cells (HUMSC, AC340316) was purchased from American Type Culture Collection (Manassas, VA). Cell Counting Kit-8 (CCK-8), Live/Dead cell staining kits, Alexa Flour 488 phalloidin and 2-(4-Amidinophenyl)-6-indolecarbamidine dihydrochloride (DAPI) were obtained from Biyuntian Biotechnology CO., Ltd. (Shanghai, China). All the chemicals were analytically pure, which was used without further purification.

2.2 | Synthesis of methacrylated gelatin (GelMA)

The preparation of GelMA follows the reported method in the literature with slight modification.³⁸ Briefly, 10 g of gelatin was dissolved 100 ml of 50°C preheated deionized water. Then, 6 ml of MA reagent was slowly dripped into the gelatin solution, the final solution was stirred for 12 h. The reaction was performed in darkness, a white milky solution was obtained after the completion of the reaction. The obtained solution was centrifuged for at 6000 rpm for 5 min and the supernatant was dialyzed in a dialysis bag (14-kDa molecular weight

cutoff) against distilled water at 40°C for 6 days. Finally, the solution was freeze-dried to obtain white porous foam-like GelMA prepolymer and stored it in a refrigerator at −20°C for later use.

2.3 | Synthesis of methacrylated sericin (SerMA)

Sericin was extracted from natural silkworm cocoon through the high heat/alkaline degumming method according to a previously reported procedure with minor modifications.³⁹ Briefly, 40 g of cocoons were cut into small pieces and boiled in Na₂CO₃ solution (1 L, 0.02 M) for 1 h. Then, the insoluble residue was removed by miracloth and the resultant solution was dialyzed (MWCO, 3500 Da) against distilled water for 3 days. Sericin was then obtained by lyophilization.

SerMA was synthesized following previously published protocols.⁴⁰ A 10 g of sericin was dissolved 100 ml of deionized water. Then, 6 ml of MA reagent was slowly dripped into the sericin solution and the pH was adjusted to 9.0 with 2 M NaOH during the reaction. After stirring for 1 h at room temperature, the pH of the solution was stabilized at 7.0 using 1 M HCl. Then, the insoluble residue was removed by miracloth and the resultant solution was dialyzed (MWCO, 3500 Da) against distilled water for 3 days. Finally, SerMA are obtained by lyophilization and stored it in a refrigerator at −20°C for later use.

2.4 | Preparation of GelMA/SerMA hydrogel

The concentration of GelMA was fixed at 20% (w/v) in deionized water, and varying amounts of SerMA (5%, 10%, and 15% [w/v]) were dissolved in deionized water. The two solutions were then mixed at a volume ratio 1:1, and LAP was added at 0.1% (w/v). The mixtures were exposed to a UV light (365 nm) at a power density of 5 mW/cm² for 30 s to produce GelMA/SerMA hydrogels.

2.5 | Characterization of polymers

The chemical structure of GelMA and SerMA was characterized by ¹H NMR (Bruker 400 MHz NMR spectrometer). The chemical construction of GelMA and SerMA was characterized by Fourier transform infrared spectroscopy (FTIR; ThermoScientific, Waltham, USA). The micromorphology of GelMA and GelMA/SerMA hydrogels was observed by scanning electron microscopy (SEM; S-3400, Hitachi, Japan) with an accelerating voltage of 5 kV. The averaged pore diameter of was calculated using Nano measure software.

2.6 | Physical properties of hydrogels

2.6.1 | Swelling ratio

The swelling ratio of the composite hydrogel was investigated using a quality method.⁴¹ Briefly, 400 µl of hydrogel was immersed in phosphate

buffered solution (PBS) (2 ml, pH 7.4) and incubated at 37°C in an incubator. At indicated time points (2, 4, 6, 8, and 24 h), the hydrogel was taken out and weighted after wiping off all surface water with a filter paper. The swelling ratio (%) was calculated based on the following formula:

$$\text{Swelling ratio} = \frac{(W_t - W_0)}{W_0} \times 100$$

where W_0 represents the initial weight of the hydrogel and W_t means the weight of the swollen hydrogel at time t .

2.6.2 | Rheological tests

Rheological measurements of the composite hydrogel were performed using a rotated rheometer (AR 2000ex; TA Instrument, USA). In the time testing, the changes of the storage modulus (G') and loss modulus (G'') were registered over time with the frequency of 1 Hz and the shear strain of 1%. In the frequency testing, the range of frequency was 0.1–10 Hz with a shear strain of 1%.

2.6.3 | Compression test

Compression experiments were conducted on a universal testing machine (Instron5543A; Boston, USA). A volume of 600 µl of hydrogel solutions were cured for 30 s in a 48-well plate and placed at the center of the lower compression plate. The compression rate of 1 mm/min was applied, and strain level was up to ≈40% of the original height.

2.6.4 | In vitro biodegradation

The degradation of hydrogels in vitro was measured following the method reported in the literature with slight modification.^{42,43} Briefly, the prepared hydrogels were incubated PBS solution (0.01 mol/L, pH = 7.4) with or without 1000 U/ml of lysozyme at 37°C with stirring speed of 60 rpm. At indicated time points, the degraded hydrogels were taken out, washed with deionized water, weighted after freeze-drying. The weight loss rate was calculated using the following formula:

$$\text{Weight loss rate (\%)} = \frac{W_t}{W_0} \times 100$$

where W_0 represents the original weight of the lyophilized hydrogel and W_t means the weight of the lyophilized hydrogel after degradation time.

2.7 | In vitro biocompatibility assessment

L929 and HUMSC cells were used to evaluate the biocompatibility of the hydrogel materials. L929 cells were cultured in high-glucose

Dulbecco's modified eagle medium (DMEM) supplemented with 10% FBS and 1% (v/v) penicillin/streptomycin at 37°C in 5% CO₂. HUMSC cells were cultured in DMEM/F12 medium supplemented with 10% FBS and 1% (v/v) penicillin/streptomycin at 37°C in 5% CO₂.

Hydrogel samples were passed through a 0.22 µm cell filter. Hydrogels of 200 µl were placed on the 48-well plate and then exposed to 405 nm blue light for 10 s. Next, 500 µl cell suspensions of L929 (2×10^4 cells/ml) and HUMSC (2×10^4 cells/ml) were added onto the hydrogel surface cultured in the corresponding medium, respectively. After 1, 3, and 5 days culture, the cells were incubated with CCK-8 solution for 2 h to evaluate the cell viability of hydrogel groups. Live/Dead cell staining kit was performed according to manufacturer's instructions to evaluate the survival and growth of L929 and HUMSC cells in hydrogels, respectively. Meanwhile, SEM experiments of HUMSC cultured on GelMA/SerMA hydrogels at 1, 3, and 5 days were performed according to a previously reported procedure with minor modifications.⁴⁴

2.8 | Scratch assays

HUMSC cells were seeded in 24-well plates at a density of 2×10^4 cells/well to create a confluent monolayer. Then, cells were starved in serum-free medium for 24 h, and a 200-µl pipette tip was used to scratch the monolayer. Next, the cells were washed with PBS to remove debris and supplied with 500 µl of leach liquor (hydrogel: medium = 1:10, mass ratio). At each indicated time interval, cell migration was monitored and photographed. For quantification, the surface area of the scratch was measured at each time-point using IPP 6.0 software.

2.9 | HUMSC cells encapsulation

2.9.1 | Live/Dead cell imaging and viability

Briefly, 100 µl of cell suspension of HUMSC (5×10^6 cells/ml) in the logarithmic growth phase were added to 900 µl of GelMA and GelMA/SerMA pregel solution, respectively. The samples were mixed well by pipetting, placed on the 12-well plate, and then exposed to 405 nm blue light for 10 s. Next, the cell-encapsulated hydrogels were incubated in DMEM/F12 medium. After 1, 4, and 7 days culture, Live/Dead cell staining kit was used to evaluate the survival and growth of the encapsulated cells. Fluorescence images were captured using a confocal microscope (FV 3000; Olympus, Japan), and 3D reconstructed images were performed with Imaris 7.2.1 software. CCK-8 assay was used to evaluate the viability of the encapsulated cells.

2.9.2 | Cytoskeleton staining

The cell-encapsulated hydrogels were washed three times with PBS and then fixed in 4% paraformaldehyde for 0.5 h. Then, the samples

were washed three times in PBS for 5 min, permeabilized in 0.5% Triton-X-100 for 10 min, and rinsed three times in PBS for 5 min. Next, the cell-encapsulated hydrogels were incubated Tetramethyl rhodamine isothio-cyanate phalloidin for 1 h and DAPI for 10 min while protected from light. Fluorescence images were captured using a confocal microscope (FV 3000; Olympus).

2.10 | Animal model

2.10.1 | Establishment of mice endometrial damage model in vivo

All animal protocols were reviewed and approved by the Institutional Animal Care and Use Committee (IACUC) of Jinan University. Briefly, all female mice were anesthetized by intraperitoneal injection of 60 mg/kg pentobarbital. The vaginal opening of mice was perfused with PBS (Sham operation group) and 95% ethanol for 30 s (experimental groups). Next, the uterus of experimental groups was injected with 100 µl PBS (normal group), GelMA/SerMA hydrogel and HUMSC cells encapsulated GelMA/SerMA hydrogel (1×10^6 cells), respectively. Then the uterus was exposed to 405 nm blue light for 30 s. The mice were euthanized and uterine tissues were excised and sectioned or frozen at Day 21 in the diestrous stage of three estrus cycles.

2.10.2 | Estrous cycles observation

The estrous cycles of the mice were monitored daily. The vagina of the mice was aspirated and washed three times with 20 µl saline through a 200 µl pipette tip. Then, the above saline was directly smeared onto glass microscope slides to air dry. Giemsa A solution was added to stain the fixed cells for 30 s, and Giemsa B solution was added to stain the fixed cells for 2 min. Glass slides were washed well in distilled water, dried on a warmer at 50°C, imaged by microscopy (RM2016; Leica, Shanghai, China).

2.10.3 | Histological examination

The uterine tissues were fixed in 4% paraformaldehyde solution overnight, followed by dimethylbenzene, and embedded in paraffin. All tissue blocks were cut into serial 4 µm thick sections and stained with hematoxylin and eosin (H&E) and Masson's trichrome staining. Immunohistochemistry of TGF-β1 was performed according to the previous steps.⁴⁵ The pictures of the stained sections were captured using a microscope (RM2016; Leica).

2.10.4 | Immunofluorescence staining

After paraffin sections rehydrated, 4 µm-thick sections were blocked using 5% BSA, after which they were incubated with mouse

anti-CD31 (Servicebio, GB13428, 1:1000), mouse anti-CK18 (Servicebio, GB11232, 1:1000), mouse anti-Ki67 (Servicebio, GB111141, 1:1000), mouse anti-Vimentin (1:100; Abcam), and mouse anti-Caspase 3 (Servicebio, GB11009-1, 1:1000) at 4°C overnight. Next, sections were washed three times using PBS and incubated with HRP-labeled goat anti-rabbit IgG secondary antibody for 1 h at room temperature. Subsequently, the sections were washed with PBS and reacted with DAB solution. Nuclei were counterstained with DAPI. Images of sections were also collected by the inverted fluorescence microscope (TE2000-S; Nikon, Japan). Images were analyzed using IPP 6.0 software to measure the percentage of positive (red color) pixels (positive staining area).

2.10.5 | Western blot analysis

For protein extraction, the samples were homogenized in tissue protein extraction reagent. Protein concentration of supernatants was determined by the BCA protein assay kit. The 20 mg of protein per sample was separated via 10% SDS-PAGE and transferred onto PVDF membranes. Afterward, the proteins were then incubated overnight at 4°C with different primary anti-bodies: anti-CD31 (Bioss, bs-0915R, 1:1000), anti-CK18 (Servicebio, GB11232, 1:1000), anti-Vimentin (Servicebio, GB1192, 1:1000) or anti-Caspase 3 (Servicebio, GB11767C, 1:1000). Membranes were then washed three times with TBST and incubated with the HRP-conjugated anti secondary antibody. The ImageJ software was used for densitometric analyses of protein bands.

2.11 | Fertility evaluation

The fertility of each group of mice was evaluated after three estrous cycles. Briefly, the female mice naturally mated with male mice in cages, and the ratio of female-to-male mice was 2:1. At 16 days after the occurrence of vaginal suppository in female mice, the female mice were sacrificed to confirm whether they were pregnant or not.

2.12 | Statistical analysis

All data were expressed as the average value \pm standard deviation at least three independent analyses. The values of p values were calculated by independent-sample t-test or one-way analyses of variance (ANOVA) test through statistical software SPSS19.0. A value of $p < 0.05$ was defined as statistically significant: * ($p < 0.05$), ** ($p < 0.01$), and *** ($p < 0.001$).

3 | RESULTS AND DISCUSSION

3.1 | Characterization of the hydrogel

In order to form hydrogels for endometrial repair, methacrylate gelatin (GelMA) and methacrylate sericin (SerMA) polymers were synthesized

through the reaction of methacrylic anhydride with gelatin and sericin. The ^1H NMR spectrum of GelMA had two peaks at 5.42 and 5.65 ppm (Figure 1a), indicating that the methacrylic group was successfully grafted onto the molecular backbone of gelatin. The ^1H NMR spectrum of SerMA had two peaks at 5.4 and 5.51 ppm (Figure 1b), verifying the methacrylic group was successfully grafted onto the molecular backbone of sericin.

As shown in Figure 1c, Fourier-transform infrared spectroscopy (FTIR) spectra analysis was carried out for characterization of synthesized GelMA and SerMA. The spectrum of GelMA displayed the typical hydroxyl group peak at around 3249 cm^{-1} . In addition, the characteristic peak at 1631, 1539, and 1444 cm^{-1} belonging to the C=O bond (amide I), bending of N—H bond (amide II), and plane vibration of C—N and N—H (amide III), respectively. Notably, the characteristic peaks of the amide II and amide III could be observed in FTIR spectrum of GelMA, which suggested the successful formation of GelMA. The spectrum of SerMA displayed that the amide I absorption peak at 1644 cm^{-1} shifted to 1637 cm^{-1} .

As shown in Figure 1d, the synthesized GelMA/SerMA mixture hydrogel was flowing liquid before crosslinking, and gradually changes into solid phase after the UV curing. Figure 1e displayed the photographs of GelMA/SerMA with different concentration of SerMA, which were opalescent and transparent state with a smooth surface. The hydrogel morphology displayed a uniform porous network structure, which played an important role in the effective diffusion of nutrients and gases and provided a suitable moisture environment for cell growth (Figure 1f). The calculated pore size for hydrogels was 10.5 ± 6.3 , 7.1 ± 5.3 , 10.0 ± 9.9 , and $5.1 \pm 4.1\text{ }\mu\text{m}$, respectively (Figure S1).

3.2 | Swelling ratio assay

As shown in Figure 2a, the swelling degree of GelMA and GelMA/SerMA hydrogels increases with time and is stable in PBS from 8 to 24 h. All hydrogels became almost saturated after 8 h, and reach their equilibrium swelling. The swelling ratio of SerMA-free GelMA, GelMA/10%SerMA, GelMA/15%HAMA, and GelMA/20%HAMA hydrogels were $22.8\% \pm 0.6\%$, $24.5\% \pm 1.1\%$, $24.8\% \pm 0.9\%$, and $27.1\% \pm 0.7\%$, respectively. These data showed that the prepared hydrogel will not expand due to absorbing too much water in the process of tissue application in vivo, thus avoiding the damage to the surrounding tissue. The addition of SerMA slightly increased the swelling rate of the hydrogel, which may be due to more holes in GelMA/SerMA hydrogel.

3.3 | Rheological and compression analysis

Figure 2b shows the variation curve of the storage modulus (G') and the loss modulus (G'') of hydrogels with time. It can be seen that both G' and G'' do not change significantly with time, and G' has always

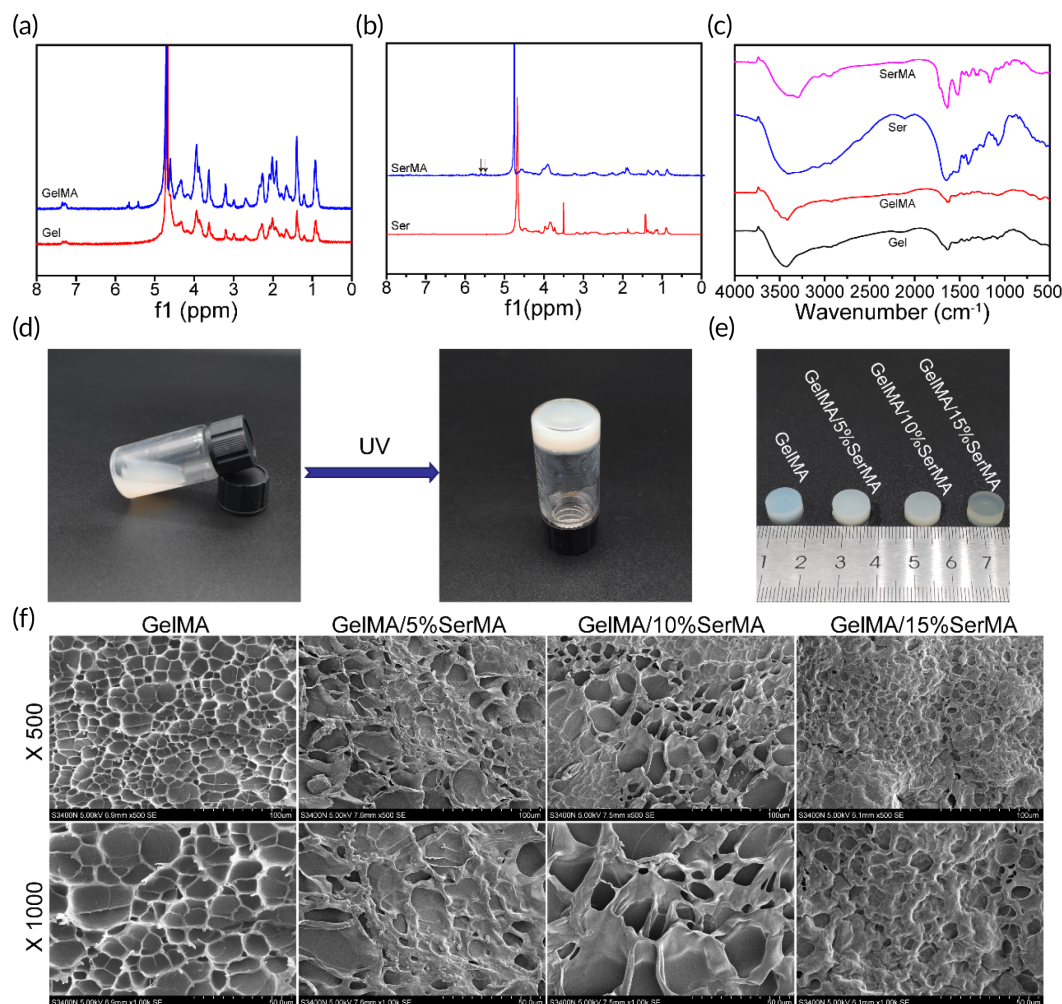


FIGURE 1 (a) ^1H NMR spectra of Gel and methacrylate gelatin (GelMA). (b) ^1H NMR spectra of Ser and SerMA. (c) Fourier-transform infrared (FTIR) spectra of Gel, GelMA, Ser, and SerMA. (d) The synthesis procedures of GelMA/SerMA. (e) The appearances of cylindrical hydrogels. (f) Structural morphology of hydrogels

been greater than G'' , indicating that the hydrogel has good stability. Meanwhile, the G' of the GelMA/SerMA hydrogel is higher than that of GelMA hydrogels, indicating that the stiffness of the GelMA/SerMA hydrogel is larger than that of GelMA hydrogels. Figure 2c showed the relationship between the G' and the G'' of the hydrogel at the rotational speed of the rheometer tray at 0.1–10 Hz. It can be found that the G' of the four kinds of hydrogel materials is larger than G'' , which indicates that the hydrogel can stably maintain its solid state at this frequency.

An ideal hydrogel for endometrial repair should equip with good mechanical properties to keep its integrity during use.⁴⁶ Figure 2d showed the test results of Young's compression modulus of hydrogel material under 40% strain. It can be found that GelMA/20%SerMA hydrogel has the largest compression modulus (118 kPa), which showed strong rigidity. Notably, the compression modulus of GelMA/10%SerMA was 40 kPa, which was more suitable for application of uterine injury and close to that of human tissues and organs.⁴⁷

3.4 | In vitro degradation

Degradation of biomaterial is one of the most important properties regarding their application in biology, which are directly related to their service life.⁴⁸ The weights of GelMA and GelMA/10%SerMA hydrogels were gradually decreased with the incubation time (Figure 3a,b). Compared to the samples of GelMA hydrogel, the samples of GelMA/10%SerMA hydrogel showed a low weight loss rate, which might due to the higher cross-linking strength. The same degradation trend also appeared in lysozyme conditions. The hydrogels were rapidly degraded when the samples were subjected to lysozyme solutions. This might be because the gelatin and sericin chains were decomposed by lysozyme.⁴⁹ These results indicated that GelMA/10%SerMA hydrogel exhibited a stable degradation rate and gradually degraded within 4 weeks, which will provide a favorable property for its application in vivo. Meanwhile, the micromorphology of freeze-dried GelMA and GelMA/10%SerMA hydrogels after degradation was shown in

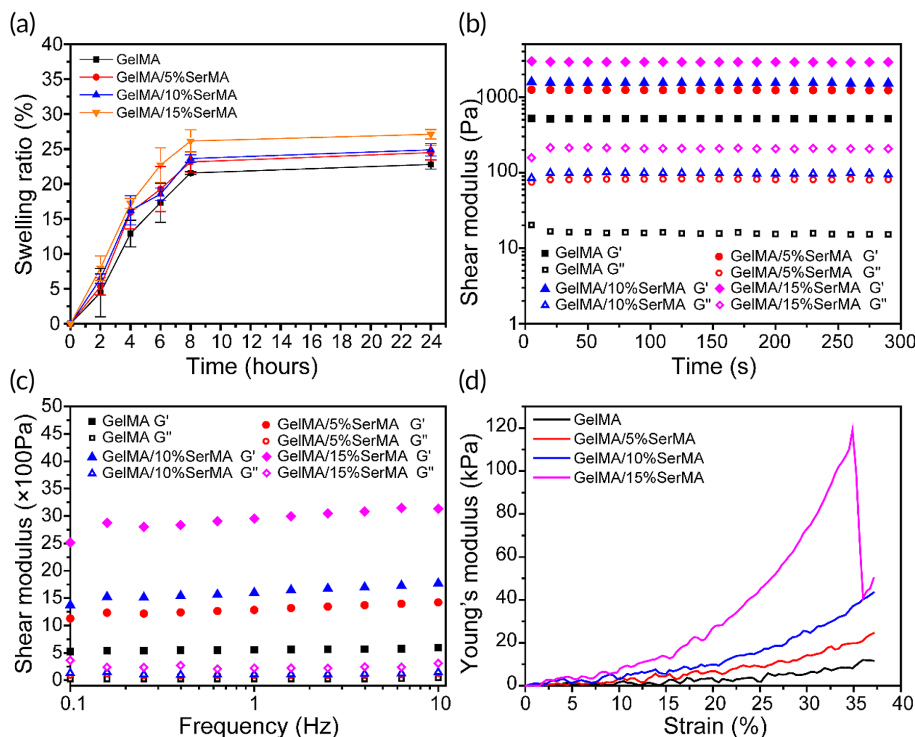


FIGURE 2 (a) The swelling ratio of hydrogels. (b) The rheological properties. (c) The hydrogel viscosity with frequency in a range between 0.1 and 100 Hz. (d) Compressive stress-strain curve

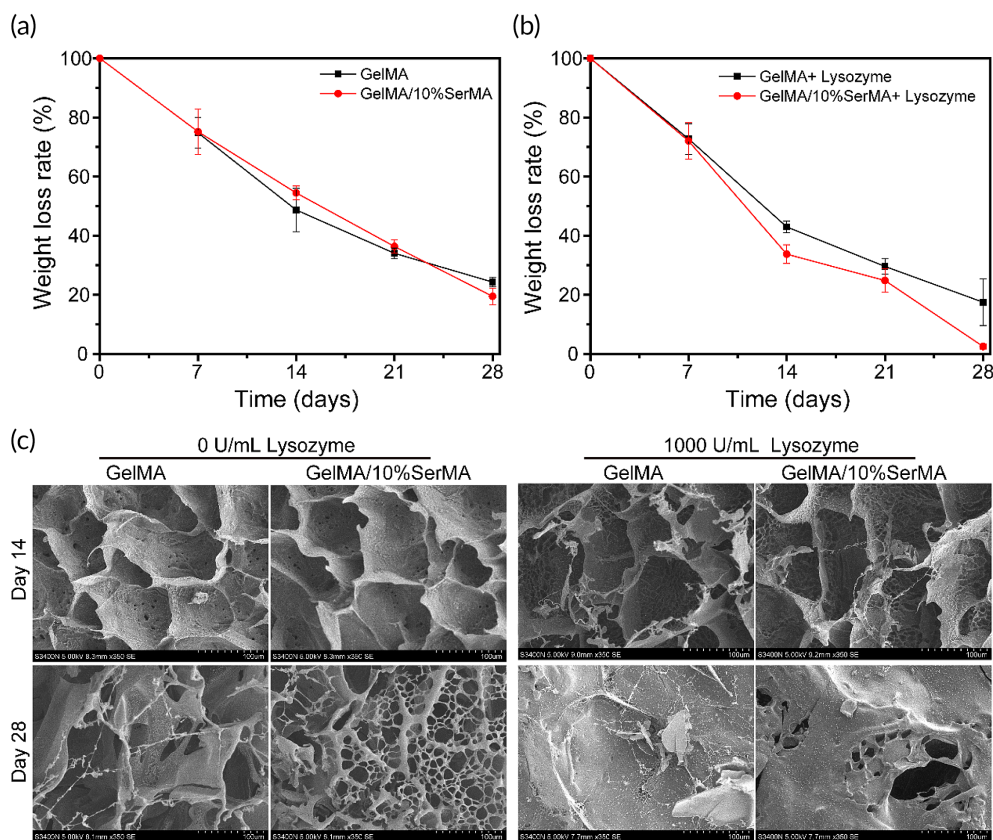


FIGURE 3 (a) The weight loss ratio of methacrylate gelatin (GelMA) and GelMA/10%SerMA hydrogels in PBS solution (0.01 mol/L, pH = 7.4) with or without 1000 U/ml of lysozyme. (b) SEM images of the surface morphology of GelMA and GelMA/10%SerMA hydrogel at Days 14 and 28

Figure 3c. In the presence of 1000 U/ml lysozyme, cracks and fragments porous structure of hydrogel were increased at Days 14 and 28, which indicated that the hydrogel was degraded with incubation time.

3.5 | Biocompatible of hydrogel

In order to study the biocompatibility of composite hydrogel, we evaluated the survival ability and proliferation effect of L929 and HUMSC

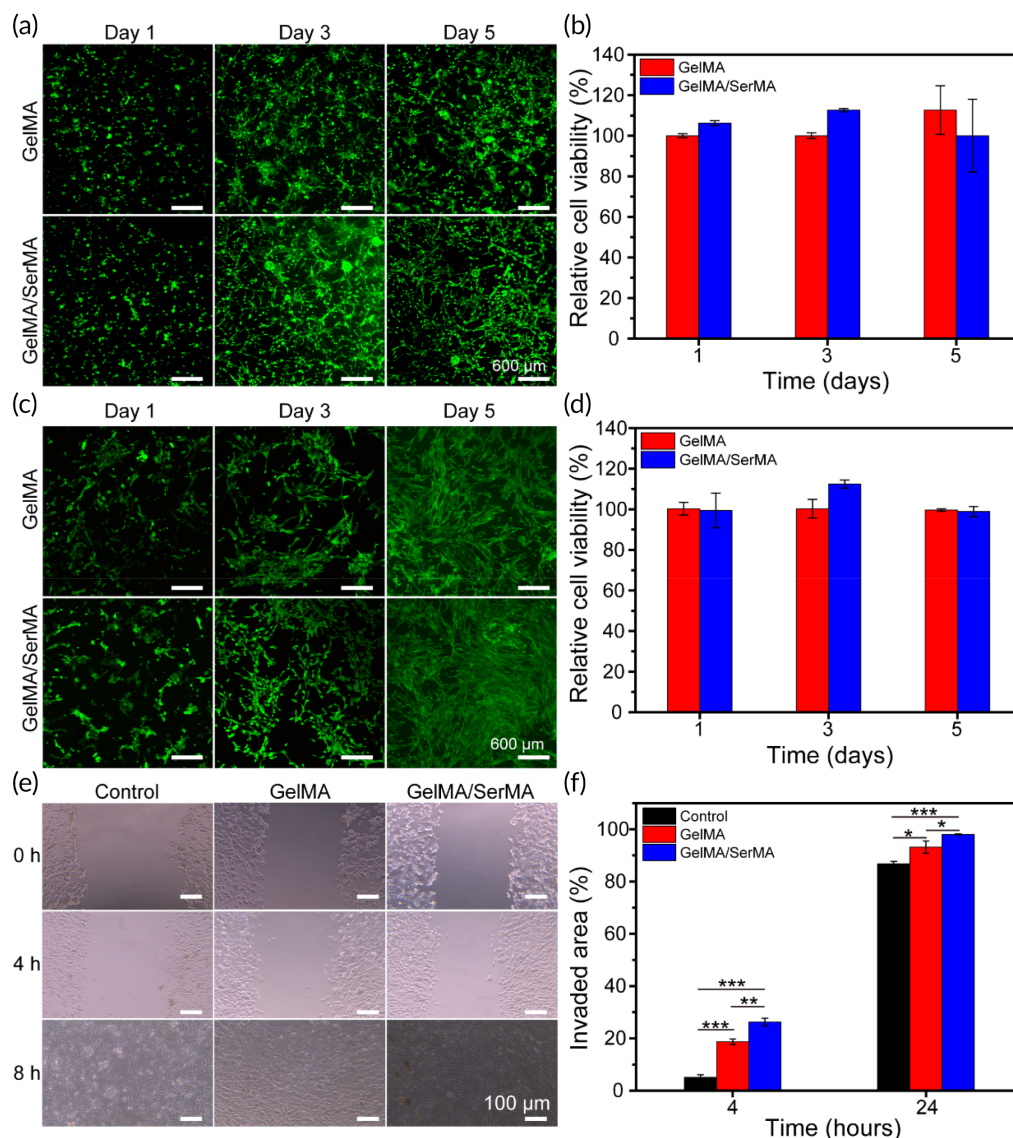


FIGURE 4 (a) Live/dead staining images of L929 cells cultured on methacrylate gelatin (GelMA), and GelMA/SerMA hydrogels at Days 1, 3, and 5. (b) Cell viability of L929 cells through CCK-8 assay at Days 1, 3, and 5. (c) Live/dead staining images of human umbilical cord mesenchymal stem cells (HUMSC) cells cultured on GelMA and GelMA/SerMA hydrogels at Days 1, 3, and 5. (d) Cell viability of HUMSC cells through CCK-8 assay at Days 1, 3, and 5. (e) Photographs showing cell migration in the hydrogel groups at 0, 4, and 8 h. (f) Quantitative analysis of invaded area. * ($p < 0.05$), ** ($p < 0.01$), and *** ($p < 0.001$)

cells on the surface of hydrogels for 1, 3, and 5 days. Calcein-AM/PI staining (green fluorescence represents living cells and red fluorescence represents dead cells) was performed. As shown in Figure 4a,c, it can be seen that L929 and HUMSC cells showed good growth and adhesion on GelMA and GelMA/SerMA hydrogels. After 3 and 5 days of culture, the survival rate of L929 and HUMSC cells in each group was higher than 90% (Figure 4b,d), and there was no significant difference ($p > 0.05$). As shown in Figure S2, the number of HUMSC cells on the GelMA/SerMA hydrogel increased with incubation time. Meanwhile, elongated cells were seen in GelMA/SerMA hydrogel. These data showed that the prepared hydrogels have good biocompatibility and cells can adhere and grow better on GelMA/SerMA hydrogels, which could be used as a biomaterial carrying cells.

The effect of GelMA and GelMA/SerMA on HUMSC cell migration was evaluated (Figure 4e). The culture medium supplemented with the same volume of PBS was used as control. For HUMSC cells, GelMA/SerMA group showed a significant increase at 4 h when compared to the control group. After incubation for 8 h, cells exposed to GelMA/SerMA group showed the highest migration ($98.0\% \pm 0.2\%$), followed by those exposed to GelMA group ($93.2\% \pm 2.3\%$) and control group ($86.8\% \pm 1.0\%$). The increased cell migration rates for cells exposed to GelMA/SerMA hydrogel are due to that sericin proteins could stimulate cell migration through inducing the expression of growth factors including platelet-derived growth factor (PDGF), vascular endothelial growth factor (VEGF), and insulin-like growth factor-1 (IGF-1).³²

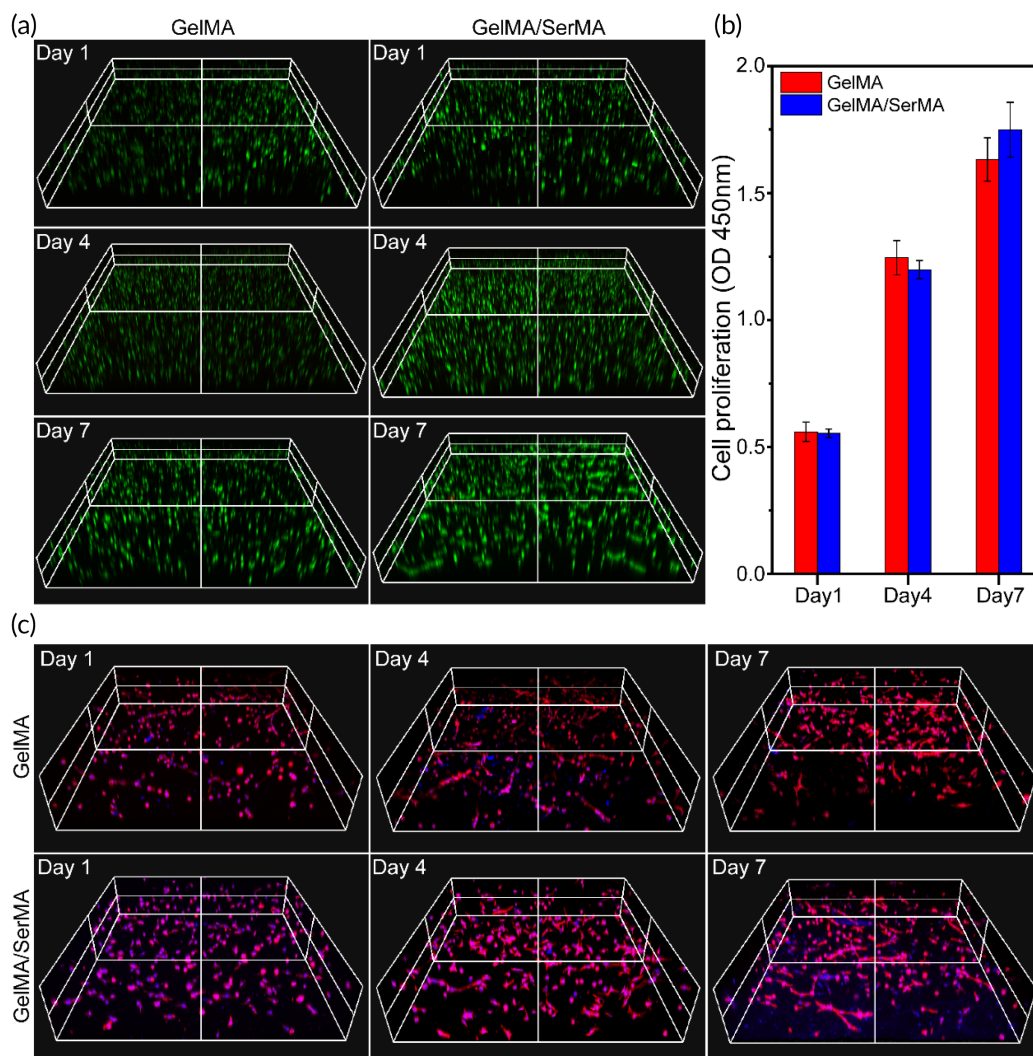


FIGURE 5 (a) Representative 3D images of encapsulated human umbilical cord mesenchymal stem cells (HUMSC) cells inside methacrylate gelatin (GelMA) and GelMA/SerMA hydrogels. (b) Proliferation of encapsulated HUMSC cells inside GelMA and GelMA/SerMA hydrogels by CCK-8 assay. (c) Cell morphology of HUMSC cells in GelMA and GelMA/SerMA hydrogels

3.6 | Cell encapsulation in hydrogel

To further evaluate whether the GelMA and GelMA/SerMA hydrogels can be served effectively as cell carriers, the encapsulation, and culture of HUMSC within hydrogels were performed. After 1, 4, and 7 days of incubation, the overall distribution of cells in hydrogels was uniform and most of the cells were alive (Figure 5a), suggesting that HUMSC cells could survive in the 3D encapsulation process. Next, the proliferation of HUMSC cells in the hydrogel was measured by CCK-8 method. Figure 5b showed that after the GelMA/SerMA hydrogel encapsulated with HUMSC cells was cultured for 1 day, the optical density (OD) value was 0.55, OD increased to 1.19 for 4 days, and the OD value continued to rise to 1.75 for 7 days. The higher OD value was due to that the gelatin and sericin materials in hydrogel are important ECM, have excellent biocompatibility and contain specific sites that bind to cells, which can promote the adhesion and proliferation of cells. As shown in Figure 5c, the morphology of HUMSC grown

on GelMA/SerMA hydrogel was different from that on GelMA hydrogel, which exhibited more elongation and thicker actin filaments. These results suggested that SerMA, as natural polymers, provided a favorable microenvironment for cell adhesion and proliferation, demonstrating that this functionalized sericin is a good candidate material for tissue engineering.

3.7 | In vivo analyses of endometrial thickness

Next, we established a mice model of endometrial injury through directly injecting 95% ethanol into the uterine horn. After modeling, the mental state of the mice in the model group and the sham operation group was normal, the diet was good and the estrous cycle was regular. As shown in Figure S3, the estrous cycle consists of four stages including proestrus (a number of nucleated epithelial cells, and a small number of keratinized epithelial cells and white blood cells),

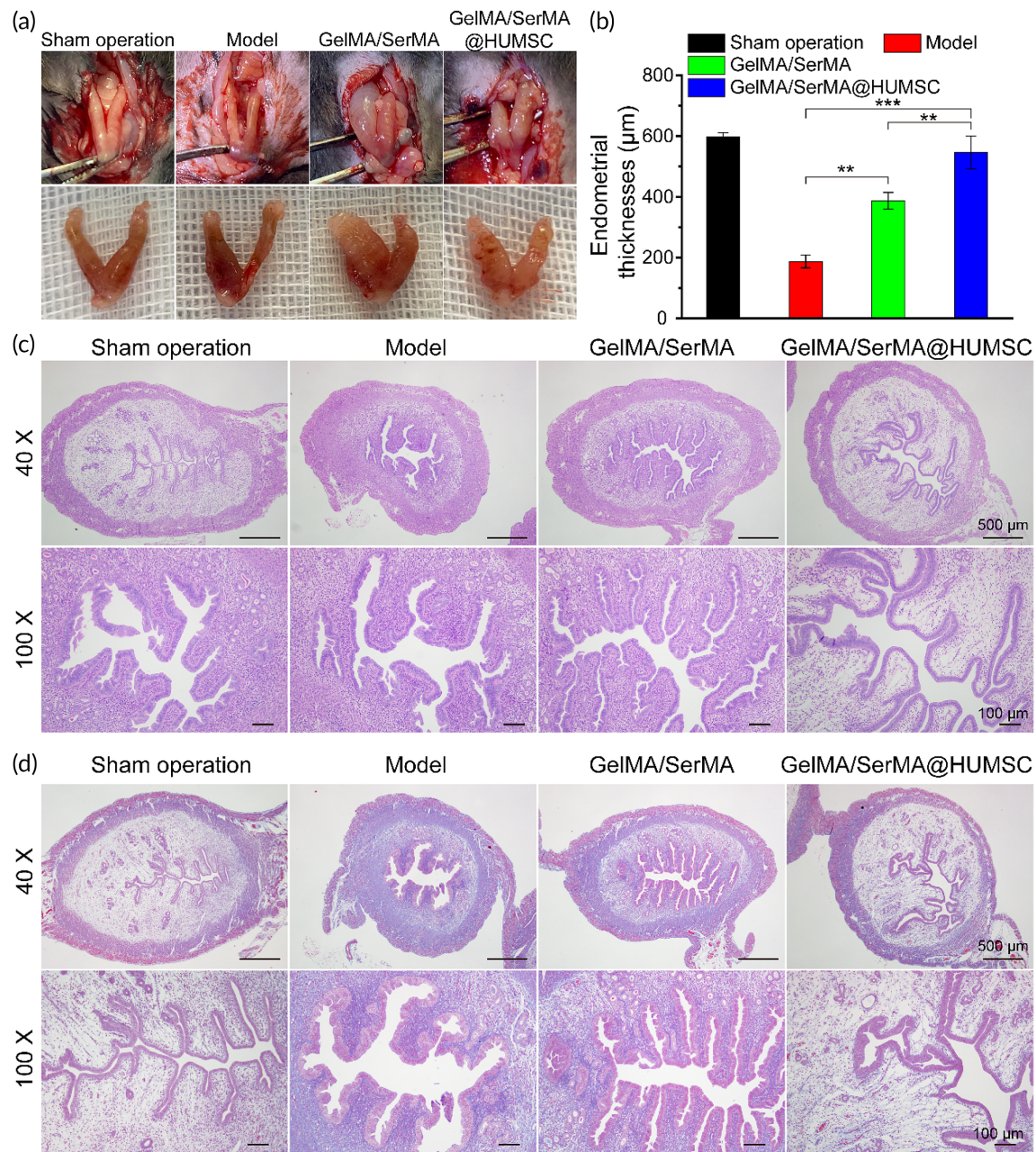


FIGURE 6 (a) The uterine status and uterine morphology of the different treatment groups (sham operation group, model group, GelMA/SerMA hydrogel group and GelMA/SerMA@HUMSC hydrogel group). (b) Quantitative analysis of endometrial thickness. (c) Representative H&E staining images of uterine samples acquired on the estrous cycles of the mice. (d) Representative Masson's trichrome staining images of uterine samples acquired on the estrous cycles of the mice. * ($p < 0.05$), ** ($p < 0.01$), and *** ($p < 0.001$)

estrus (a large number of scattered or clustered keratinized enucleated epithelial cells), metestrus (nucleated epithelial cells, enucleated epithelial cells and white blood cells), and diestrus (the cells are mainly white blood cells.).

As shown in Figure 6a, the uterine shape of the sham operation group and GelMA/SerMA@HUMSC hydrogel group is regular and uniform and elastic. The uterine shrinkage of the model group is inelastic, dark color, irregular Y shape, and viable necrotic tissue. The damaged uterine tissue showed obvious thinning of the endometrium, which is indistinguishable from the myometrium in some areas. To study the

effect of hydrogel on injured endometrium in mice, the uterine specimens of mice in each group were collected and analyzed by HE and Masson staining after three estrous cycles. The suitable thickness of endometrium can provide an excellent attachment place for embryo implantation, which is the key condition to ensure a good pregnancy outcome. The thin endometrium may affect the receptivity of endometrium and lead to the failure of embryo implantation. Therefore, the thickness of endometrium is an important index to measure whether the endometrium is repaired after injury. As shown in Figure 6b, the thickness of endometrium in the sham operation group,

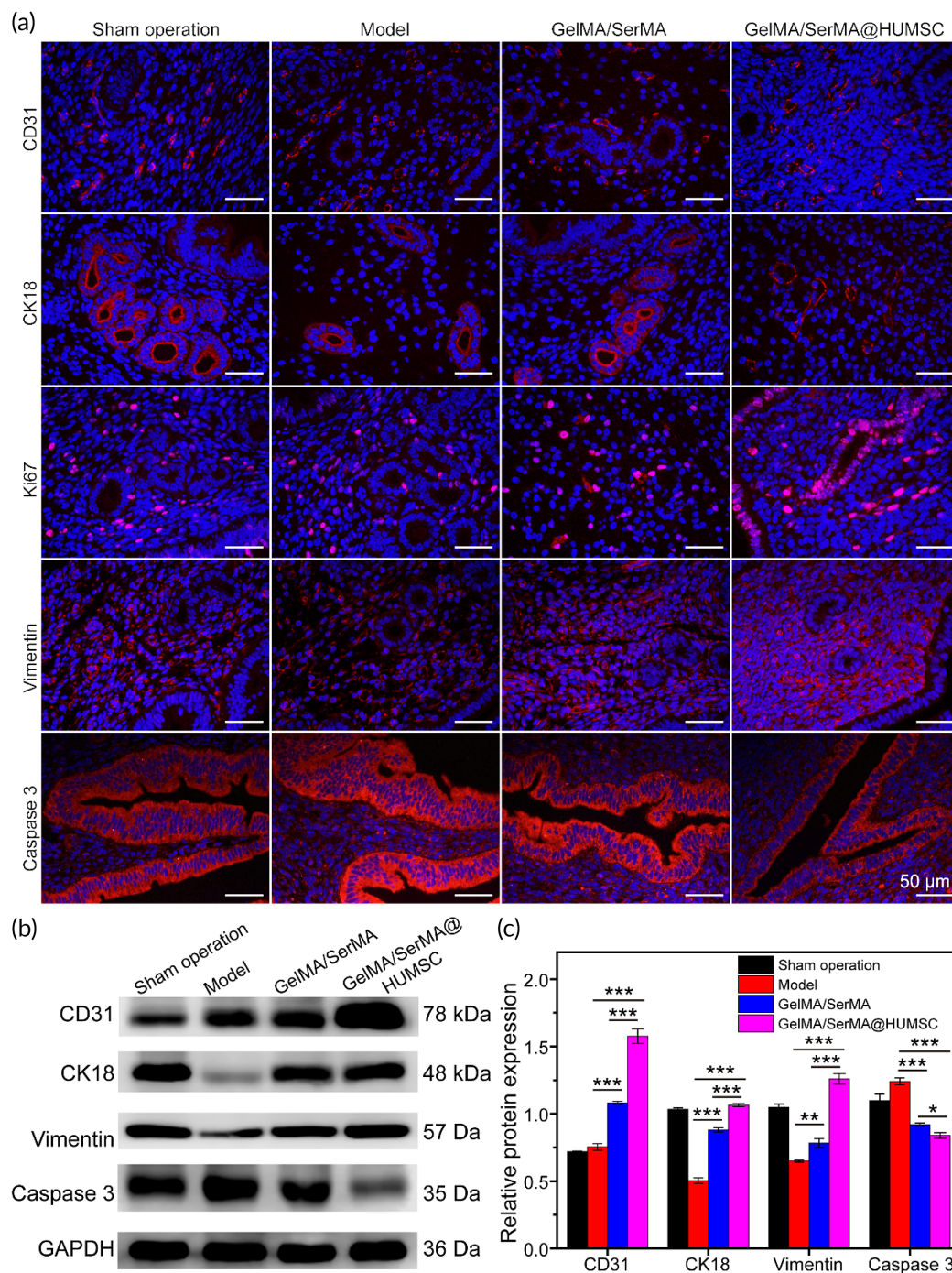


FIGURE 7 (a) Representative CD31, CK18, Ki67, Vimentin, and Caspase 3 images of immunofluorescence staining of uterine samples. (b) Western bolt analysis of CD31, CK18, Vimentin, and Caspase 3. (c) The quantitative analysis of WB data. * ($p < 0.05$), ** ($p < 0.01$), and *** ($p < 0.001$)

Model group, GelMA/SerMA hydrogel group, and GelMA/SerMA@HUMSC hydrogel group were 598.4 ± 12.8 , 187.6 ± 20.7 , 387.8 ± 27.4 , and 546.6 ± 54.2 μ m, respectively. Meanwhile, the thickness of endometrium and Gland-like structures in the GelMA/SerMA@HUMSC hydrogel were similar to that of sham operation group. Notably, the thickness of endometrium in the model group decreased significantly compared with the sham operation group. As shown in Figure 6c, the uterine cavity blockage and adhesion in the

GelMA/SerMA@HUMSC hydrogel treatment group were significantly improved compared with the model group, and the thickness of the endometrium was significantly thicker than that in the model group ($p < 0.001$). As shown in Figure 6d, the uterine tissue of the model group has numerous fibrillates. However, the fibrotic area in the GelMA/SerMA@HUMSC hydrogel treatment group showed small amounts of fibrillates, which was attributed to that HUMSC could inhibit endometrial fibrosis.⁵⁰ Transforming growth factor (TGF- β 1)

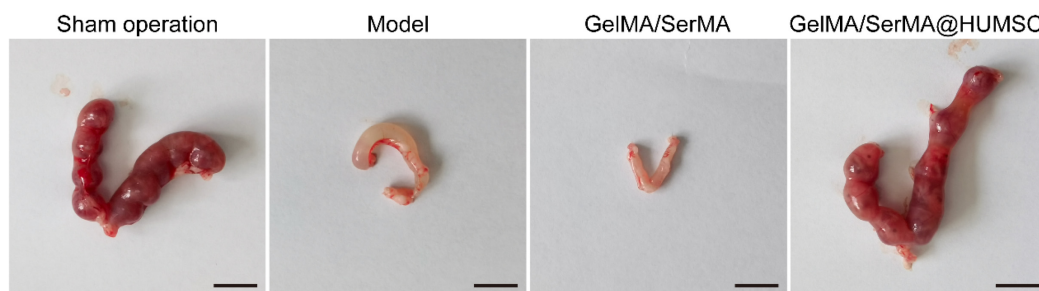


FIGURE 8 Pregnancies in the different treatment groups (sham operation group, model group, GelMA/SerMA hydrogel group and GelMA/SerMA@HUMSC hydrogel group)

was a multifunctional polypeptide cytokine, which could promote fibroblast proliferation and fibrin formation at the high expression levels, resulting in the development of endometriosis. As shown in Figure S4A,B, the expression of TGF- β 1 in the GelMA/SerMA@HUMSC hydrogel treatment group was the lowest, which indicated GelMA/SerMA@HUMSC hydrogel could improve fibrosis of endometriosis. These results showed that GelMA/SerMA@HUMSC hydrogel transplantation group could increase the thickness of endometrium and improve the endometrial interstitial fibrosis, resulting in promoting the repair of injured endometrium.

3.8 | Immunofluorescence staining

Uterine receptivity is regulated by a number of factors that coordinate intrauterine changes facilitate blastocyst implantation. Next, we evaluated the expression of differentiation 31 (CD31), cytokeratin 18 (CK18), cell proliferation antigen Ki-67 (Ki67), Vimentin, and Caspase 3, which are widely studied markers of endometrial receptivity and play multiple roles in a series of related developmental processes.

CD31 is an important index to evaluate neovascularization.⁵¹ As shown in Figure 7a, the distribution of CD31 in the sham operation group was more than that in the model group, while the expression of CD31 in the GelMA/SerMA hydrogel treatment group was between the sham operation group and the model group. As shown in Figure S5A, the CD31 positive ratio of sham operation group, model group, GelMA/SerMA hydrogel group, and GelMA/SerMA@HUMSC hydrogel group were $8.2\% \pm 1.0\%$, $15.4\% \pm 1.4\%$, $13.8\% \pm 0.6\%$, and $23.9\% \pm 2.5\%$, respectively. CK18 is member of the keratin family of intermediate filament proteins, which is more expressed in the cytoplasm of endometrial epithelial cells.⁵² As shown in Figure S5B, the expression of CK18 in the sham operation group is more than that in the model group, while that in the model group is less. The expression of CK18 in the GelMA/SerMA hydrogel treatment group and the GelMA/SerMA@HUMSC hydrogel treatment group is more than that in the model group, indicating that the efficacy in the hydrogel treated group is better than that in the model group.

Ki67 is an important index to evaluate cell proliferation.⁵³ There is more proliferation in the sham operation group and less in the model

group. As shown in Figure S5C, the expression of Ki67 in the GelMA/SerMA hydrogel treatment group and the GelMA/SerMA@HUMSC hydrogel treatment group is more than that in the model group, indicating better cell proliferation and tissue growth. Vimentin is an indicator of the specific expression of Vimentin in endometrial stromal cells.⁵⁴ As shown in Figure S5D, the expression of CK18 in the sham operation group is more than that in the model group, while the expression of CK18 in the GelMA/SerMA hydrogel treatment group and the GelMA/SerMA@HUMSC hydrogel treatment group is more, and the expression effect is the same as that in the sham operation group, indicating that the combination of hydrogels with HUMSC may achieve better therapeutic effect. Caspase-3 activation is a hallmark of apoptotic cell death. As shown in Figure S5E, the expression of Caspase 3 in GelMA/SerMA hydrogel treatment group and the GelMA/SerMA@HUMSC hydrogel treatment group. As shown in Figure 7b,c, western blot analysis showed a similar trend.

3.9 | Fertility evaluation

To study the effect of hydrogel transplantation on the fertility of mice with endometrial injury, hydrogel was transplanted into the uterine cavity of mice after modeling, and female mice and male mice were mated in cages after three estrous cycles. As shown in Figure 8, the implantation number was the highest in the sham operation group after cage mating. Compared with the model group, the implantation number in the GelMA/SerMA@HUMSC hydrogel group was significantly higher than those in the model group. All data showed GelMA/SerMA@HUMSC hydrogel can promote functional endometrial regeneration and facilitate the recovery of fertility, which could regulate endometrial regeneration through the use of multifunctional hydrogels. Prior study demonstrated that stem cell transplantation can improve the fertility of rats with damaged endometrium and support fertilized egg implantation and embryonic development.⁵⁰

4 | CONCLUSION

In this study, we have developed an injectable hydrogel based on methacrylate gelatin (GelMA) and methacrylate sericin (SerMA) matrix

as cell delivery carriers of HUMSC to promote angiogenesis and endometrial regeneration, thus promoting the recovery of fertility. The swelling, mechanical, and degradation properties of GelMA/SerMA hydrogel could be regulated by adjusting the concentration of SerMA. In vitro results showed that the GelMA/SerMA hydrogel could promote the proliferation and migration of HUMSC and have good cell encapsulation ability. On mice endometrial damage model in vivo, the GelMA/SerMA@HUMSC hydrogel could increase the thickness of endometrium and improve endometrial interstitial fibrosis through upregulating the expression of CD31, CK18, Ki67 and Vimentin, and downregulating the expression of Caspase 3, resulting in promoting the repair of injured endometrium. Therefore, local use of hydrogel with stem cell encapsulation is a promising method to enhance endometrial regeneration and improve pregnancy outcome.

ACKNOWLEDGMENTS

This research is supported by the Regional Joint Fund of basic and Applied basic Research Fund of Guangdong Province (2019B151520082). Foshan Municipal Science and Technology Bureau 2020 Foshan Municipal Science and Technology Research Project (2020001006077). Special funding Fund for Clinical Scientific Research of Wu Jieping Medical Foundation (320.6750.18101; 320.6750.2021-04-43.).

AUTHOR CONTRIBUTIONS

Lixuan Chen: Conceptualization (equal); methodology (equal); writing - original draft (equal). **Ling Li:** Methodology (equal); writing - original draft (equal). **Qinglin Mo:** Data curation (equal); investigation (equal); methodology (equal). **Xiaomin Zhang:** Data curation (equal); formal analysis (equal); methodology (equal). **Chaolin Chen:** Data curation (equal); formal analysis (equal); methodology (equal). **Yingnan Wu:** Formal analysis (equal); methodology (equal); software (equal). **Xiaoli Zeng:** Methodology (equal); resources (equal). **Kaixian Deng:** Data curation (equal); methodology (equal); resources (equal). **Nanbo Liu:** Data curation (equal); methodology (equal); resources (equal). **Ping Zhu, Mingxing Liu and Yang Xiao:** Conceptualization, Methodology, Formal analysis, Data curation, Writing - review & editing, Supervision, Funding acquisition.

CONFLICT OF INTERESTS

The authors declare no competing financial interest.

PEER REVIEW

The peer review history for this article is available at <https://publons.com/publon/10.1002/btm2.10328>.

DATA AVAILABILITY STATEMENT

Some or all data, models, or code generated or used during the study are available from the corresponding author by request.

ORCID

Yang Xiao  <https://orcid.org/0000-0003-0046-4967>

REFERENCES

1. Wilson M, Reske J, Holladay J, et al. ARID1A and PI3-kinase pathway mutations in the endometrium drive epithelial transdifferentiation and collective invasion. *Nat Commun*. 2019;10:3554.
2. Corachán A, Pellicer N, Pellicer A, Ferrero H. Novel therapeutic targets to improve IVF outcomes in endometriosis patients: a review and future prospects. *Hum Reprod Update*. 2021;27:923-972.
3. Wang L, Yu C, Chang T, et al. In situ repair abilities of human umbilical cord-derived mesenchymal stem cells and autocrosslinked hyaluronic acid gel complex in rhesus monkeys with intrauterine adhesion. *Sci Adv*. 2020;6:eaba6357-eaba.
4. Ding L, Li X, Sun H, et al. Transplantation of bone marrow mesenchymal stem cells on collagen scaffolds for the functional regeneration of injured rat uterus. *Biomaterials*. 2014;35:4888-4900.
5. Kim S, Kim Y, Kim H, Ku S. Animal models closer to intrauterine adhesive pathology. *Ann Transl Med*. 2020;8:1125.
6. Murta M, Machado RC, Zegers-Hochschild F, Checa MA, Sampaio M, Geber S. Endometriosis does not affect live birth rates of patients submitted to assisted reproduction techniques: analysis of the Latin American network registry database from 1995 to 2011. *J Assist Reprod Genet*. 2018;35:1395-1399.
7. Ji W, Hou B, Lin W, et al. 3D bioprinting a human iPSC-derived MSC-loaded scaffold for repair of the uterine endometrium. *Acta Biomater*. 2020;116:268-284.
8. Liu F, Hu S, Wang S, Cheng K. Cell and biomaterial-based approaches to uterus regeneration. *Regen Biomater*. 2019;6:141-148.
9. Park S, Park HH, Sun K, et al. Hydrogel Nanospine patch as a flexible anti-pathogenic scaffold for regulating stem cell behavior. *ACS Nano*. 2019;13:11181-11193.
10. Kim YY, Park KH, Kim YJ, et al. Synergistic regenerative effects of functionalized endometrial stromal cells with hyaluronic acid hydrogel in a murine model of uterine damage. *Acta Biomater*. 2019;89:139-151.
11. Rahmani A, Saleki K, Javanmehr N, Khodaparast J, Saadat P, Nouri HR. Mesenchymal stem cell-derived extracellular vesicle-based therapies protect against coupled degeneration of the central nervous and vascular systems in stroke. *Ageing Res Rev*. 2020;62:101106.
12. Li J, Narayanan K, Zhang Y, et al. Role of lineage-specific matrix in stem cell chondrogenesis. *Biomaterials*. 2020;231:119681.
13. Wang W, Tan B, Chen J, et al. An injectable conductive hydrogel encapsulating plasmid DNA-eNOs and ADSCs for treating myocardial infarction. *Biomaterials*. 2018;160:69-81.
14. Park S, Kim S, Park C, et al. Sonic hedgehog, a novel endogenous damage signal, activates multiple beneficial functions of human endometrial stem cells. *Mol Ther*. 2020;28:452-465.
15. Khan Z, Goldberg JM. Hysteroscopic management of Asherman's syndrome. *J Minim Invasive Gynecol*. 2018;25:218-228.
16. Marinaro F, Gómez-Serrano M, Jorge I, et al. Unraveling the molecular signature of extracellular vesicles from endometrial-derived mesenchymal stem cells: Potential modulatory effects and therapeutic applications. *Front Bioeng Biotechnol*. 2019;7:431.
17. Yuan FY, Zhang MX, Shi YH, et al. Bone marrow stromal cells-derived exosomes target DAB2IP to induce microglial cell autophagy, a new strategy for neural stem cell transplantation in brain injury. *Exp Ther Med*. 2020;20:2752-2764.
18. Syed SM, Kumar M, Ghosh A, et al. Endometrial Axin2(+) cells drive epithelial homeostasis, regeneration, and cancer following oncogenic transformation. *Cell Stem Cell*. 2020;26:64-80.e13.
19. Han J, Kim YS, Lim MY, et al. Dual roles of graphene oxide to attenuate inflammation and elicit timely polarization of macrophage phenotypes for cardiac repair. *ACS Nano*. 2018;12:1959-1977.
20. Zhou F, Hong Y, Liang R, et al. Rapid printing of bio-inspired 3D tissue constructs for skin regeneration. *Biomaterials*. 2020;258:120287.

21. Zhao L, Weir MD, Xu HH. An injectable calcium phosphate-alginate hydrogel-umbilical cord mesenchymal stem cell paste for bone tissue engineering. *Biomaterials*. 2010;31:6502-6510.
22. Li X, Zhang C, Haggerty AE, et al. The effect of a nanofiber-hydrogel composite on neural tissue repair and regeneration in the contused spinal cord. *Biomaterials*. 2020;245:119978.
23. Magalhaes R, Williams J, Yoo K, Yoo J, Atala A. A tissue-engineered uterus supports live births in rabbits. *Nat Biotechnol*. 2020;38:1280-1287.
24. Xie T, Ding J, Han X, et al. Wound dressing change facilitated by spraying zinc ions. *Mater Horizons*. 2020;7:605-614.
25. Kim SW, Kim YY, Kim H, Ku SY. Recent advancements in engineered biomaterials for the regeneration of female reproductive organs. *Reprod Sci*. 2021;28:1612-1625.
26. Llorens-Gómez M, Salesa B, Serrano-Aroca Á. Physical and biological properties of alginate/carbon nanofibers hydrogel films. *Int J Biol Macromol*. 2020;151:499-507.
27. Tuan HNA, Nhu VTT. Synthesis and properties of pH-Thermo dual responsive semi-IPN hydrogels based on N,N'-Diethylacrylamide and Itaconamic acid. *Polymers (Basel)*. 2020;12:1139.
28. Urbani L, Camilli C, Phylactopoulos DE, et al. Multi-stage bioengineering of a layered oesophagus with in vitro expanded muscle and epithelial adult progenitors. *Nat Commun*. 2018;9:4286.
29. Haque A, Hexig B, Meng Q, Hossain S, Nagaoka M, Akaike T. The effect of recombinant E-cadherin substratum on the differentiation of endoderm-derived hepatocyte-like cells from embryonic stem cells. *Biomaterials*. 2011;32:2032-2042.
30. Ma D, Zhao Y, Huang L, et al. A novel hydrogel-based treatment for complete transection spinal cord injury repair is driven by microglia/macrophages repopulation. *Biomaterials*. 2020;237:119830.
31. Gao F, Xu Z, Liang Q, et al. Osteochondral regeneration with 3D-printed biodegradable high-strength supramolecular polymer reinforced-gelatin hydrogel scaffolds. *Adv Sci (Weinh)*. 2019;6:1900867.
32. Chouhan D, Mandal BB. Silk biomaterials in wound healing and skin regeneration therapeutics: from bench to bedside. *Acta Biomater*. 2020;103:24-51.
33. Reddy R, Jiang Q, Aramwit P, Reddy N. Litter to leaf: the unexplored potential of silk byproducts. *Trends Biotechnol*. 2021;39:706-718.
34. Ai L, He H, Wang P, et al. Rational design and fabrication of ZnONPs functionalized Sericin/PVA antimicrobial sponge. *Int J Mol Sci*. 2019;20:4796-4810.
35. Wang Y, Cai R, Tao G, et al. A novel AgNPs/Sericin/agar film with enhanced mechanical property and antibacterial capability. *Molecules*. 2018;23(7):1821.
36. Sultan MT, Choi BY, Ajiteru O, et al. Reinforced-hydrogel encapsulated hMSCs towards brain injury treatment by trans-septal approach. *Biomaterials*. 2021;266:120413.
37. Neves SC, Moroni L, Barrias CC, Granja PL. Leveling up hydrogels: hybrid systems in tissue engineering. *Trends Biotechnol*. 2020;38:292-315.
38. Corbett DC, Fabian WB, Grigoryan B, et al. Thermofluidic heat exchangers for actuation of transcription in artificial tissues. *Sci Adv*. 2020;6:eabb9062.
39. Qi C, Deng Y, Xu L, et al. A sericin/graphene oxide composite scaffold as a biomimetic extracellular matrix for structural and functional repair of calvarial bone. *Theranostics*. 2020;10:741-756.
40. Qi C, Liu J, Jin Y, et al. Photo-crosslinkable, injectable sericin hydrogel as 3D biomimetic extracellular matrix for minimally invasive repairing cartilage. *Biomaterials*. 2018;163:89-104.
41. Dooling LJ, Tirrell DA. Engineering the dynamic properties of protein networks through sequence variation. *ACS Cent Sci*. 2016;2:812-819.
42. Kim YH, Yang X, Shi L, et al. Bisphosphonate nanoclay edge-site interactions facilitate hydrogel self-assembly and sustained growth factor localization. *Nat Commun*. 2020;11:1365.
43. Ke X, Li M, Wang X, et al. An injectable chitosan/dextran/ β -glycerophosphate hydrogel as cell delivery carrier for therapy of myocardial infarction. *Carbohydr Polym*. 2020;229:115516.
44. Lu K, Li K, Zhang M, et al. Adipose-derived stem cells (ADSCs) and platelet-rich plasma (PRP) loaded gelatin/silk fibroin hydrogels for improving healing in a murine pressure ulcer model. *Chem Eng J*. 2021;424:130429.
45. Wang H, Shen L, Sun X, et al. Adipose group 1 innate lymphoid cells promote adipose tissue fibrosis and diabetes in obesity. *Nat Commun*. 2019;10:3254.
46. Lv H, Wu B, Song J, Wu W, Cai W, Xu J. Hydrogel, a novel therapeutic and delivery strategy, in the treatment of intrauterine adhesions. *J Mater Chem B*. 2021;9:6536-6552.
47. Wei S, Xu P, Yao Z, et al. A composite hydrogel with co-delivery of antimicrobial peptides and platelet-rich plasma to enhance healing of infected wounds in diabetes. *Acta Biomater*. 2021;124:205-218.
48. Wei J, Jia J, Wu F, et al. Hierarchically microporous/macroporous scaffold of magnesium-calcium phosphate for bone tissue regeneration. *Biomaterials*. 2010;31:1260-1269.
49. Xu Y, Patsis PA, Hauser S, et al. Cytocompatible, injectable, and Electroconductive soft adhesives with hybrid covalent/noncovalent dynamic network. *Adv Sci (Weinh)*. 2019;6:1802077.
50. Lin J, Wang Z, Huang J, et al. Microenvironment-protected exosome-hydrogel for facilitating endometrial regeneration, fertility restoration, and live birth of offspring. *Small (Weinheim an der Bergstrasse, Germany)*. 2021;17:e2007235.
51. Robotti F, Sterner I, Bottan S, et al. Microengineered biosynthesized cellulose as anti-fibrotic in vivo protection for cardiac implantable electronic devices. *Biomaterials*. 2020;229:119583.
52. Zhang H, Zhao H, Wang X, Cui X, Jin L. Keratin 86 is up-regulated in the uterus during implantation, induced by oestradiol. *BMC Dev Biol*. 2020;20:3.
53. Alonso R, Flament H, Lemoine S, et al. Induction of anergic or regulatory tumor-specific CD4(+) T cells in the tumor-draining lymph node. *Nat Commun*. 2018;9:2113.
54. Liu H, Zhang Z, Xiong W, et al. Long non-coding RNA MALAT1 mediates hypoxia-induced pro-survival autophagy of endometrial stromal cells in endometriosis. *J Cell Mol Med*. 2019;23:439-452.

SUPPORTING INFORMATION

Additional supporting information may be found in the online version of the article at the publisher's website.

How to cite this article: Chen L, Li L, Mo Q, et al. An injectable gelatin/sericin hydrogel loaded with human umbilical cord mesenchymal stem cells for the treatment of uterine injury. *Bioeng Transl Med*. 2023;8(1):e10328. doi:[10.1002/btm2.10328](https://doi.org/10.1002/btm2.10328)